Site preference of Fe atoms in $FeMgSiO_4$ and $FeMg(SiO_3)_2$ studied by density functional calculations

Swastika Chatterjee,[1] Surajit Sengupta,[2,*] and Tanusri Saha-Dasgupta[1,†]
[1]*Department of Material Sciences, S. N. Bose National Center for Basic Sciences, JD-III, Salt Lake City, Kolkata 700 098, India*
[2]*Department of Chemical, Biological, and Macro-Molecular Sciences, S. N. Bose National Center for Basic Sciences, JD-III, Salt Lake City, Kolkata 700 098, India*

Koustav Chatterjee and Nibir Mandal
Indian Institute of Science Education and Research, IIT Kharagpur Extension Centre, Block-HC, Sector-III, Salt Lake City, Kolkata 700106, India
(Received 4 November 2008; published 5 March 2009)

Using first-principles density functional calculation we investigate site preference of Fe in $FeMgSiO_4$ olivine and $FeMg(SiO_3)_2$ pyroxene, which are the major constituents of the earth's upper mantle. A combination of state-of-the-art methods has been used for this purpose. The strong correlation effect at Fe site has been taken care of by means of local-density approximation+U calculations, and the crystal structures have been optimized by means of total-energy calculations. Our $T=0$ K study in the total-energy-minimized structures indicate a strong preference for Fe to occupy $M2$ site in case of pyroxene and a preference for Fe to occupy $M1$ site in case of olivine. We provide the microscopic understanding of our finding in terms of density of states and charge densities.

DOI: 10.1103/PhysRevB.79.115103 PACS number(s): 71.20.Be, 91.32.Gh

I. INTRODUCTION

Silicate minerals are the building blocks of earth. Out of a wide variety of silicate minerals, olivine and pyroxene are the predominant mineral phase present in the earth's upper mantle. Knowledge of physical and chemical properties of these minerals is of great geophysical interest as they record the physicochemical environment prevailing at great depths. The olivine group incorporates a range of closely associated anhydrous minerals characterized by orthorhombic symmetry and a general formula M_2SiO_4 where M can be divalent cations such as Fe^{2+}, Mg^{2+}, Ca^{2+}, Co^{2+}, Ni^{2+}, or Mn^{2+}. Most of the natural olivines can be considered as the solid solution series between the Mg-rich end member forsterite (Mg_2SiO_4) and the Fe-rich end member Fayalite (Fe_2SiO_4). Apart from terrestrial rocks, they also occur in meteorites and other extra terrestrial planetary materials. Thus, these mineral phases have drawn great attention of workers from different branches of earth and planetary sciences over several decades. A principal objective of these studies aims at developing thermodynamical models and uses them to understand thermal evolution and differentiation processes in the mantle. Pyroxene with a general formula $M_2(SiO_3)_2$, where M=Mg, Fe, Ca, and Na, is another important silicate phase in the earth. It crystallizes either in the monoclinic or orthorhombic system. The basic structural units in both olivines and pyroxenes are the same. They consist of Si-O tetrahedron and M-O octahedron. These octahedral units are further of two types, namely, $M1$ and $M2$. The $M1$ octahedron geometry is comparatively more regular and smaller in size, whereas $M2$ octahedron is more distorted and larger.

A problem of great geological importance is the nature of site preference of Fe-Mg in orthorhombic olivines and pyroxenes. At a given temperature, Fe and Mg cations are partitioned into the two octahedral sites $M1$ and $M2$ with varying proportions. It is an experimentally established fact that at room temperatures Fe prefers to occupy $M2$ site in pyroxenes, resulting in enrichment of Mg in $M1$ site.[1,2] In contrary, there is a wide variation in results on site preference in olivine. Earliest studies on the distribution of Fe-Mg over the two nonequivalent sites in olivines date back to 1960s.[3] Several investigations using x-ray diffraction,[4] Mossbauer spectroscopy,[5] and crystal-field spectra[6] yielded information about the crystal structure of olivine and suggested that the Fe^{2+}-Mg^{2+} distribution is either random or weakly ordered, with Fe^{2+} preferring $M2$ site, which is a general tendency of Fe^{2+} observed in other silicate group of minerals. However, some experimental studies conducted on terrestrial and lunar samples of natural olivine revealed tendency of Fe^{2+} to occupy $M1$ sites.[7] These studies measured the distribution coefficient, $K_D=(\mathrm{Mg/Fe})M1/(\mathrm{Mg/Fe})M2$, to deduce the site preference of Fe-Mg over the octahedral sites and concluded that K_D value increase with rising temperature indicating ordering of Fe^{2+} in the smaller and more regular $M1$ site. Since then a variety of experimental as well as theoretical studies[8] employing parameters such as temperature,[9] kinematics of Mg-Fe cation exchange between $M1$ and $M2$ sites,[10] pressure,[11] fugacity of oxygen,[12] and presence of elements other than Fe-Mg at octahedral sites[13] were carried out to resolve the contradiction. These experimental results, however failed to reach a common conclusion. *In situ* neutron-diffraction studies conducted on olivine[14] reveals a switch over in the trend of K_D value with increasing temperature, suggesting a reversal of preference of Fe^{2+} from $M1$ to $M2$ at a critical temperature. These findings were challenged by latter studies, which emphasize on ordering of Fe^{2+} into smaller $M1$ site with increasing temperature.[15]

The study of intracrystalline partitioning of Fe and Mg into the two octahedral sites can greatly help in the thermodynamic modeling of earth's mantle and also in understand-

TABLE I. The Wyckoff positions for each species in case of olivine.

Atom	Class	Coordinates
*M*1	4*a*	(0,0,0), (1/2,1/2,0), (0,0,1/2), (1/2,1/2,1/2)
*M*2, Si, O1, and O2	4*c*	$(x,y,1/4)$, $(x+1/2,-y+1/2,3/4)$, $(-x,-y,3/4)$, $(-x+1/2,y+1/2,1/4)$
O3	8*d*	(x,y,z), $(x+1/2,-y+1/2,-z)$, $(-x,-y,z+1/2)$, $(-x+1/2,y+1/2,-z+1/2)$, $(-x,-y,-z)$, $(-x+1/2,y+1/2,z)$, $(x,y,-z+1/2)$, $(x+1/2,-y+1/2,z+1/2)$

ing planetary processes. Before one attempts in understanding the complex temperature dependence and the thermodynamic evolution of the site preference, it is worthwhile to consider the $T=0$ K case and investigate the site preference issue from a quantum-mechanical point of view, which to the best of our knowledge has not been attempted before. Hence in this present work we have conducted extensive studies based on first-principles electronic structure calculations to resolve the nature of Fe-Mg distribution in olivines. We have used pyroxene as a benchmark to justify and establish our methodology, for which the site preference of Fe has been definitely established.

The rest of the paper is organized as follows: we first present a structural comparison between olivine and pyroxene in Sec. II. This is followed up by the computational details in Sec. III. Section IV consists of results. Finally we present our conclusions in Sec. V.

II. CRYSTAL STRUCTURE

Olivines with a general formula M_2SiO_4 crystallize in the orthorhombic space group *Pbnm* (international table No. 62). The unit cell contains four formula units containing 28 atoms: 8 Fe/Mg, 4 Si, and 16 O. The corresponding Wyckoff positions are given in Table I. Orthopyroxenes too crystallize in the orthorhombic symmetry with a space group of *Pbca* (international table No. 61). The unit cell contains 8 formula units consisting of 80 atoms in the unit cell: 16-cations(Fe/Mg), 16 Si, and 48 O, with all species occupying Wyckoff position 8*c*.

In order to understand the complex crystal structure of these silicate minerals we break up the complete lattice structure into three sublattices: (i) Si-O tetrahedral unit, (ii) M1-O octahedral unit, and (iii) M2-O octahedral unit and compare them for olivine and pyroxene (Fig. 1).

A. Si-O tetrahedral unit

All silicates including olivine and pyroxene are essentially built out of $(SiO_4)^{4-}$ tetrahedral building blocks (see left panels in Fig. 1). In any $(SiO_4)^{4-}$ unit there are three distinct oxygen positions corresponding to three distinct Si-O bonds. Out of the four oxygen two oxygen ions are equidistant from Si. These are labeled as O3. The oxygen farthest from Si^{4+} is O1. It forms the apical oxygen in SiO_4 unit. The remaining one situated nearest to Si^{4+} is O2. In olivines the tetrahedral units are completely isolated from each other, i.e., they are so-called nesosilicates. Viewed on the *bc* plane (top left panel in Fig. 1), the tetrahedral units form rows parallel to *c* axis with alternately pointing up and down along the *b* axis in any particular row. On the other hand orthopyroxenes

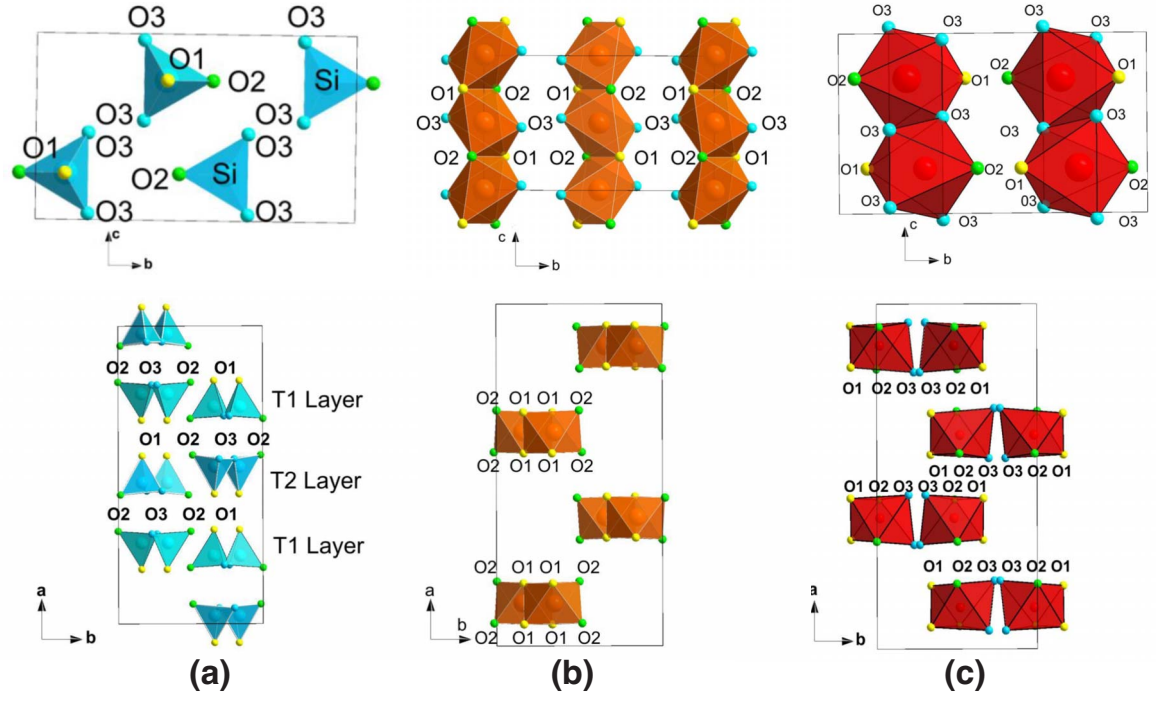

FIG. 1. (Color online) Building units of olivine projected onto *bc* plane (top panel) and pyroxene projected onto *ab* plane (bottom panel). (a) SiO_4 tetrahedral unit. (b) *M*1-O octahedral unit. (c) *M*2-O octahedral unit.

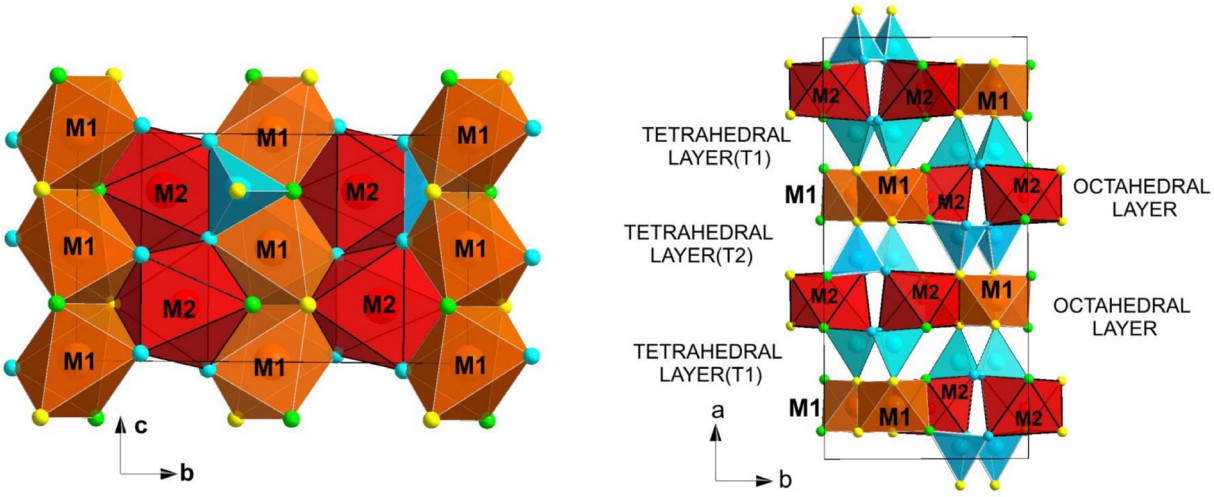

FIG. 2. (Color online) Complete lattice structure of olivine (left panel) and pyroxene (right panel).

are the so-called inosilicate or chain silicate (bottom left panel in Fig. 1). Any $(SiO_4)^{4-}$ unit shares its two O3 oxygen with the neighboring $(SiO_4)^{4-}$ units forming a chain along c axis. These chains are not straight as obvious from the view along c (bottom left panel in Fig. 1) but form layer of tetrahedral units parallel to bc plane. These alternate planes can be further distinguished as T1 and T2 layer. The three distinct oxygen belonging to T1 are regarded as O1A, O2A, and O3A, and those belonging to T2 are designated as O1B, O2B, and O3B.

B. *M*1-O octahedral unit

In both olivine and pyroxene $M1$ octahedral units are connected to each other in such a way so that they form chains. In olivine, there are two O1, two O2, and two O3 oxygen atoms that form the $M1O_6$ octahedral unit along with central $M1$. The neighboring $M1O_6$ octahedral units share edges (O1-O2) to form chains parallel to c axis (top middle panel in Fig. 1). In pyroxene, there are two O1A, two O1B, one O2A, and one O2B surrounding $M1$ that form the $M1O_6$ octahedra. It is to be noticed that O3A and O3B are not connected to $M1$. The $M1O_6$ octahedra share (O1A-O2B) edges with adjacent $M1$ octahedral units to form zigzag chain such as structures running almost parallel to c axis.

C. *M*2-O octahedral unit

There are one O1, one O2, and four O3 oxygen atoms that form the $M2O_6$ octahedron in olivine. A $M2O_6$ octahedral unit is connected to surrounding four $M2$ octahedral units by sharing O3 oxygen atoms to form a somewhat corrugated plane parallel to ac face of the unit cell. In case of pyroxene, $M2O_6$ octahedral unit built by one each of O1A, O2A, O3A, O1B, O2B, and O3B surrounding the central $M2$ ion remains completely isolated from another $M2O_6$ octahedra.

On superimposing the three sublattices, one obtains the full structure of olivines and pyroxenes as shown in Fig. 2.

III. METHODOLOGY

In order to investigate the electronic properties of olivine and pyroxene, we have used density functional theory (DFT) (Ref. 16) within the framework of local-density approximation (LDA). For our DFT calculations we considered a combination of two different methods, namely, a plane-wave-based method as implemented in the Vienna *ab initio* Simulation Package (VASP) (Ref. 17) and muffin-tin orbital (MTO) based linear muffin-tin orbital (LMTO) method[18] as implemented in Stuttgart TBLMTO-47 code. The plane-wave-based VASP method was used for structural minimization, while the electronic structures in the energy-minimized crystal structures were calculated using both LMTO and plane-wave basis sets. The accuracy of the electronic structure calculations within the scheme of the two methods have been checked with respect to each other. For plane-wave calculations we have used projector augmented wave (PAW) potentials[19] and the wave functions were expanded in the plane-wave basis with a kinetic-energy cutoff of 500 eV. Reciprocal space integration was carried out with a k mesh of $7\times7\times7$.

In order to take into account the missing correlation effect beyond LDA, which turns out to be important for the proper description of Fe-derived states we have carried out LDA $+U$ (Ref. 20) (where U is the on-site Coulomb repulsion) calculations within the self-interaction double-counting correction (SIC).[21] We also performed calculations with the around mean-field (AMF) correction in order to check the influence of double-counting correction. Our conclusions remained unchanged.

The total-energy calculations for Fayalite (Fe_2SiO_4) at various U values, in the range 4–5 eV with an interval of 0.5, within the plane-wave-based basis were carried out for getting the minimum energy crystal structure. We found a strong effect of U in the structural optimization with a minimum of energy obtained for $U=4.5$ eV, an effect which has been also observed before.[22]

For all the calculations reported in the following, we have fixed the value of U at 4.5 eV, while the Hund's exchange J

TABLE II. Optimized structural parameters for olivine and pyroxene where all $M1$ ($M2$) sites are occupied by Fe (Mg) and vice versa in comparison to experimentally determined structure (data taken from Refs. 21 and 22). Lattice constants have been kept fixed at the experimental values.

OLIVINE

				Optimized data					
	Experimental data[a]			Fe at $M1$			Fe at $M2$		
Atom	x	y	z	x	y	z	x	y	z
$M1$	0	0	0	0	0	0	0	0	0
$M2$	0.992	0.279	0.25	0.992	0.278	0.25	0.987	0.278	0.25
Si	0.425	0.098	0.25	0.428	0.096	0.25	0.429	0.094	0.25
O1	0.768	0.092	0.25	0.75	0.095	0.25	0.767	0.088	0.25
O2	0.217	0.451	0.25	0.208	0.448	0.25	0.226	0.451	0.25
O3	0.283	0.164	0.035	0.284	0.165	0.035	0.284	0.163	0.033

PYROXENE

				Optimized data					
	Experimental data[b]			Fe at $M1$			Fe at $M2$		
Atom	x	y	z	x	y	z	x	y	z
$M1$	0.375	0.654	0.874	0.376	0.656	0.863	0.376	0.655	0.874
$M2$	0.378	0.483	0.367	0.376	0.492	0.358	0.378	0.487	0.366
Si1	0.474	0.337	0.796	0.473	0.336	0.708	0.473	0.336	0.796
Si2	0.272	0.341	0.052	0.274	0.341	0.049	0.272	0.341	0.058
O1	0.562	0.337	0.799	0.562	0.34	0.790	0.562	0.335	0.798
O2	0.312	0.501	0.053	0.314	0.5	0.041	0.313	0.501	0.056
O3	0.447	0.204	0.595	0.448	0.195	0.597	0.447	0.199	0.597
O4	0.184	0.338	0.041	0.185	0.344	0.027	0.183	0.337	0.046
O5	0.435	0.484	0.696	0.431	0.48	0.683	0.433	0.485	0.695
O6	0.303	0.231	0.824	0.304	0.21	0.832	0.303	0.228	0.833

[a]Reference 24.
[b]Reference 25.

is chosen to be 0.8 eV (introduced to consider the multiorbital situation.)

IV. RESULTS

A. Structural optimization

We have performed structural minimization in case of olivines and pyroxenes. This is done in order to obtain the most stable configuration as crystal structure data used are for actual minerals which might have been formed under various diverse conditions and hence might not be the minimum energy structure. Moreover O positions cannot be very accurately estimated using x-ray diffraction. Hence a structural optimization was done by employing the plane-wave pseudopotential method using VASP code. The atomic positions have been optimized keeping the lattice constants fixed at the experimentally estimated values.

The structural parameters, as obtained in our calculations are summarized in Table II. While the experimental measurements do not report separate data for Fe occupying $M1$ and $M2$ sites, the energy-optimized data do depend on whether Fe occupies $M1$ or $M2$ site. We have therefore carried out structural relaxations for the two individual cases, where Fe occupies $M1$ and $M2$ sites, respectively. Table II shows the structural data for representative cases where all the $M1$ ($M2$) sites are occupied by Fe (Mg) and vice versa. The energetically optimized atomic positions show reasonable agreement in comparison to experimental data listed in the first three columns. While the position of Fe/Mg cations and Si atom are found to remain more or less unchanged, the O atomic positions are found to differ at most by 5% for olivine and 10% for pyroxene. In the following, we have considered for our calculations the energetically optimized structure in each case.

B. Basic electronic structure

A non-spin-polarized DFT-LDA calculation shows both Fe containing olivine and pyroxene to be insulators. The insulating solution as obtained in non-spin-polarized LDA calculations can be rationalized in the following manner: the octahedral surrounding of Fe splits the Fe d states into t_{2g} and e_g. The non-spin-polarized calculation forces Fe^{2+} ($3d^6$) to go into low spin configuration, i.e., the t_{2g} levels are completely filled, whereas the e_g levels are completely empty.

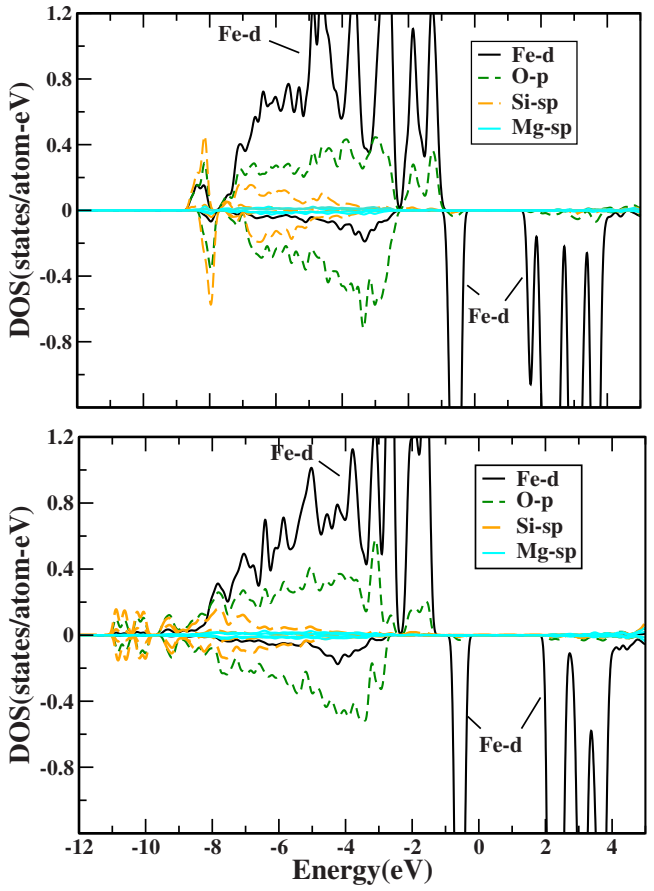

FIG. 3. (Color online) Partial DOSs of olivine (top panel) and pyroxene (bottom panel) projected onto Fe d, O p, Si, and Mg. Within each panel the upper(lower) subpanel corresponds to majority (minority) spin. The negative of DOS has been plotted for the minority channel for clarity.

The splitting between the t_{2g}-e_g levels appears as the gap at the Fermi level, while the Mg and Si derived states arising out of nominal Mg^{2+} and Si^{4+} configurations remain empty, thereby providing the insulating solution. However, relaxation of spin degrees of freedom through spin-polarized calculations find Fe in its high spin state, with a finite magnetic moment of about $3.7\mu_B$ at the Fe site. The spin-polarized calculation within the framework of LDA yields a metallic solution with fully filled Fe d states in the majority-spin channel and partially filled Fe t_{2g} states in the minority spin channel. It is therefore expected that the inclusion of missing correlation effect in LDA, within the partially filled Fe t_{2g} manifold would lead to opening up of a gap through formation of Mott-Hubbard insulator. The LDA+U calculations confirm this expectation.

Figure 3 presents the LDA+U density of state (DOS) for olivine ($FeMgSiO_4$) and pyroxene [$FeMg(SiO_3)_2$] projected on to Fe d, O p, Mg sp, and Si sp states. The zero of the energy is set at the top of the valence band. In the calculations one of the octahedral sites has been assumed to be occupied by Fe and the rest by Mg. We show the density of states for the representative cases where the Fe (Mg) atoms have been put at $M1$ ($M2$) sites since the gross features of the density of states remain the same in different site occupancies. As is seen from the DOS plot (Fig. 3), while the Mg and Si states remain empty with negligible contribution in the occupied part of the DOS, the occupied part of the DOS and the density of states close to Fermi energy is dominated by O p and Fe d derived states, indicating the strong hybridization between Fe d and O p. The d-p hybridized bands extend from −9 to 4 eV in case of olivine and −11–5 eV in case of pyroxene. The split out states at the bottom of dp derived manifold in case of pyroxene in the energy range of about −11 to −9 eV arises out of O3A and O3B oxygen which remain disconnected to $M1$ site.

TABLE III. LDA+U total energies for olivine and pyroxene with Fe atoms placed at the $M1$ sites and $M2$ sites, respectively. Energy differences between the two configurations are listed in the last row.

Olivine		Pyroxene	
Site	Energy (eV)	Site	Energy (eV)
Fe at $M1$	−218.041 33	Fe at $M1$	−644.2392
Fe at $M2$	−217.89932	Fe at $M2$	−645.4710
Energy difference per Fe=35.5 meV(412 K)		Energy difference per Fe=154.0 meV(1787 K)	

C. Total-energy calculations: Site preference

The total-energy calculations within the framework of LDA+U carried out in optimized geometries for olivine and pyroxene is shown in Table III for 50-50 concentration of Fe and Mg. We find that in case of pyroxene when Fe is in the $M2$ site the total energy is much lower compared to when it occupies the $M1$ site, the energy difference being 154 meV (1787 K) per Fe site.[23] Hence this should be the stable preferred configuration. This finding is in accordance with published experimental results, where a significant preference of Fe to order into the $M2$ site has been reported. Having succeeded in arriving at the correct description of site preference in case of pyroxene, we extend our methodology to olivine where the situation is rather unsettled. In the case of olivine our total-energy calculations show a preference for $M1$ site, the energy difference being 35.5 meV (412 K) per Fe site.

Total-energy calculations performed at lower concentrations of Fe in olivine, i.e., 25% (two Fe atoms per unit cell) and 12.5% (one Fe atom per unit cell) also show a preference of Fe for $M1$ site. For 25% concentration of Fe we obtain a energy difference of 44 meV (511 K) per Fe atom, whereas for 12.5% concentration, the energy difference is found to be 60 meV (696 K) per Fe atom. The quoted values are obtained by taking the average of energy differences where the two Fe sites are placed at six different configurations in case of 25% concentration and four different configurations in case of 12.5% concentration.

Further, attempts made to simulate the hydrostatic pressure by varying the experimentally measured lattice constant at ambient pressure do not seem to alter the conclusion of Fe preferentially occupying $M1$ site. The energy difference was

TABLE IV. Size and structural distortion of octahedral units.

Site	Average *M*-O bond length (Å)	Volume of MO_6 octahedron $(Å)^3$	rms deviation of *M*-O bond length (Å)
	Olivine		
*M*1	2.1287	12.8612	0.0407
*M*2	2.1611	13.4575	0.078
	Pyroxene		
*M*1	2.0917	12.2022	0.0592
*M*2	2.2029	14.2536	0.1842

found to change by about 3% for a change in lattice parameters by 2%.

D. Discussion

Structural analysis presented in Table IV shows that the distortion of $M2O_6$ octahedral unit in case of olivine is about two times larger than that of $M1O_6$, while it is three times larger in case of pyroxene. The size consideration shows $M2O_6$ octahedra to be 17% larger in volume compared to $M1O_6$ in case of pyroxene, while it is only 5% larger in case of olivine. The structural difference between $M1O_6$ and $M2O_6$ octahedra is therefore much larger in case of pyroxene compared to olivine. The ionic radius of Fe^{2+}(0.76 Å) is 0.04 Å large compared to that of Mg^{2+}(0.72 Å). The mere size consideration would hence imply Fe^{2+} to preferentially occupy *M*2 site both in case of pyroxene and olivine. Our total-energy calculations on the other hand indicate Fe^{2+} occupies *M*1 site in case of olivine and *M*2 site in case of pyroxene. So while the simple size consideration works for pyroxene with a large structural difference between *M*1 and *M*2 sites, it fails for the case of olivine where the structural difference between *M*1-*M*2 sites is small. We note that the size argument is based on the concept of isolated $M1O_6$ and $M2O_6$ octahedra and does not take into account the connectivity of *M*1 and *M*2 sites to other sites which is different between olivine and pyroxene and should be an important parameter in the determination of site preference.

In the following, in order to unravel the microscopic origin of site preferences we consider the comparison of density of states where the Fe sites have been put into *M*1 or *M*2 site (Fig. 4). While the gross features of the density of states are found to be similar between *M*2 occupied Fe^{2+} and *M*1 occupied Fe^{2+} situations, with occupied part of the spectrum being dominated by O *p* and Fe *d*, the two densities of states differ in fine details. The difference between DOSs in *M*1 and *M*2 occupied cases appear to be more pronounced in case of pyroxene than in case of olivine, which is in agreement with larger structural difference between *M*1 and *M*2 in case of pyroxene compared to olivine. The DOS shows a band gap of 2.18 eV for olivine with Fe occupying *M*1 site as compared to a band gap of 2.16 eV with Fe occupying *M*2 site. In contrast, for pyroxene the band gap is found to be 3.06 eV for Fe in *M*2 site and 2.30 eV for Fe in *M*1 site. Larger band-gap points toward greater stability in terms of lowering of band energy. The lowering of energy levels can happen through increased covalency effect between metal *d* and *p* levels of neighboring oxygen sites. In case of pyroxene, the *M*1 site is connected to four oxygen sites out of

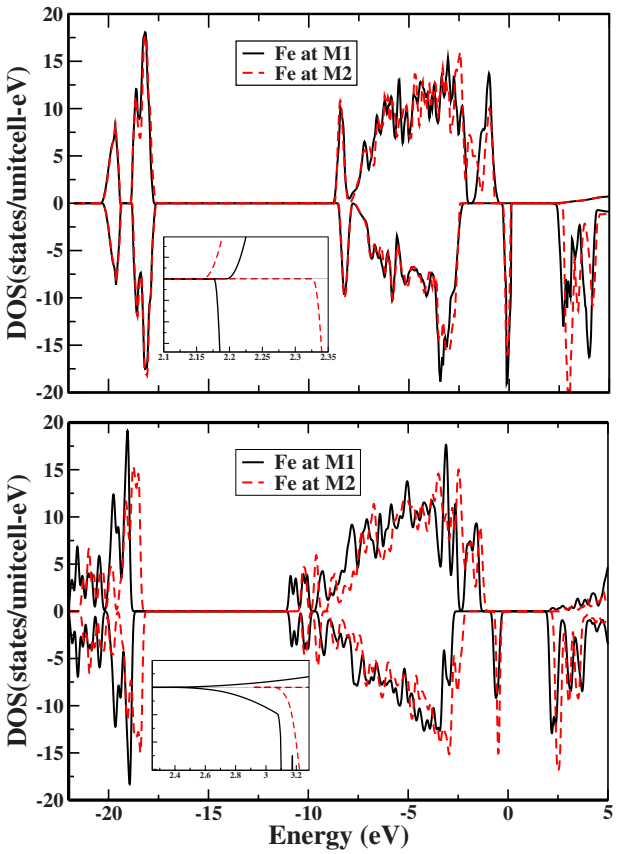

FIG. 4. (Color online) Comparison between total DOSs for olivine and pyroxene with Fe at *M*1 and *M*2 sites in olivine (top panel) and pyroxene (bottom panel). The solid and the dashed lines correspond to DOS for Fe at *M*1 and *M*2, respectively. Inset shows an enlarged plot of DOS focused at the bottom of the conduction band.

available six inequivalent O sites, while $M2$ site is connected to all the oxygen. The enhanced covalency effect for $M2$ site therefore works hand in hand with the larger volume effect at $M2$ site which results into distinct preference of Fe^{2+} to go into $M2$ site. In case of olivine, the $M1$ site forms chains by sharing the oxygen edges of neighboring octahedra, while $M2$ sites form a network with corner-shared oxygen from neighboring octahedra with reduced connectivity. This causes enhanced covalency in case of $M1$ occupied situation which is found to be sufficient enough to overcome the size preferred $M2$ occupied situation. Figure 5 shows the charge-density plots in ac plane for olivine with $M1$ sites occupied by Fe (top panel) and $M2$ sites occupied by Fe (bottom panel). The Fe-O covalency is found to be much stronger for the $M1$ occupied case compared to $M2$ occupied case, corroborating further the arguments presented above.

V. CONCLUSION

In conclusion, we have carried out a thorough study of the site preference problem in case of silicate minerals such as olivine and pyroxene using first-principles electronic structure calculations within the framework of density functional theory. While the experimental situation clearly indicates a preference for $M2$ site over $M1$ site for Fe in case of pyroxene, the situation in case of olivine is debatable. Our calculations at $T=0$ K from a purely quantum chemical point of view found a strong preference toward $M2$ site for pyroxene in agreement with experimental finding, while at $T=0$ K preference toward $M1$ site has been found for olivines. Our study finds the important role of covalency in deciding the site preference in addition to size effect. We believe, our zero-temperature results will form the basis of future finite temperature calculations in this system. Specifically, the problem of interest concerns the possible change in site preference of the Fe^{2+} ions in olivine as a function of temperature as reported in the literature. In order to study the reaction Fe^{2+} $(M1) \rightleftharpoons Fe^{2+}$ $(M2)$ in detail, we need to obtain the energy barriers for such exchange mechanism from first-principles calculations, from which reaction rates and site occupancy as a function of temperature may be obtained. Calculations in this direction are currently in progress which will be communicated in the near future.

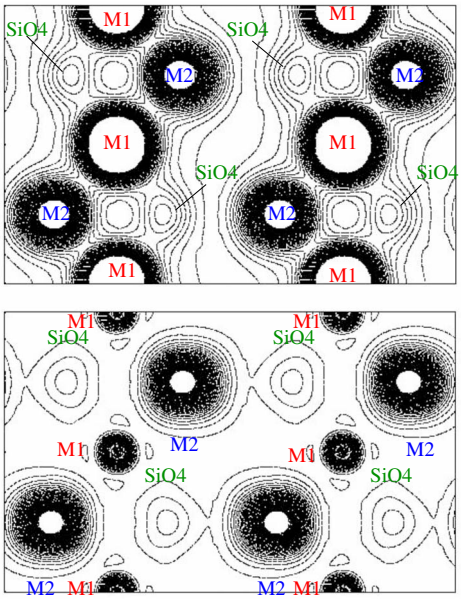

FIG. 5. (Color online) Charge-density plot of olivine projected onto the ac plane. Top panel shows Fe at $M1$ site and Mg at $M2$ site. Bottom panel shows Fe at $M2$ site and Mg at $M1$. Contour values are $\rho_n = \delta \times n \times e^-/(\text{a.u})^3$, where $\delta = 0.002$ and n labels the contours. Note enhanced covalency for Fe at $M1$ (top panel) compared to Fe at $M2$ (bottom panel).

ACKNOWLEDGMENTS

We thank the funding through Advanced Materials Research Unit. The authors also acknowledge Shweta Sagnewar for her involvement at the initial stage of the project.

*Present address: Centre for Advanced Materials, Indian Association for the Cultivation of Science, Jadavpur, Kolkata 700032, India.

†Corresponding author: tanusri@bose.res.in

[1] J. A. Sykes-Nord and G. M. Molin, Am. Mineral. **78**, 921 (1993).

[2] G. M. Molin, S. K. Saxena, and E. Brizi, Earth Planet. Sci. Lett. **105**, 260 (1991).

[3] S. Ghosh, Am. Mineral. **47**, 388 (1962).

[4] J. D. Birle, G. V. Gibbs, P. B. Moore, and J. V. Smith, Am. Mineral. **53**, 807 (1968).

[5] W. R. Bush, S. S. Hafner, and D. Virgo, Nature (London) **227**, 1339 (1970).

[6] R. G. Burns, Am. Mineral. **55**, 1609 (1970).

[7] L. W. Finger, Year Book - Carnegie Inst. Washington **69**, 302 (1971); H. R. Wenk and K. N. Raymond, Z. Kristallogr. **137**, 86 (1973); J. R. Smyth and R. M. Hazen, Am. Mineral. **58**, 588 (1973); S. Ghosh, C. Wan, and I. S. McCallum, Indian J. Earth Sci. **3**, 1 (1976).

[8] H. Annersten, J. Adetunji, and A. Filippidis, Am. Mineral. **69**, 1110 (1984); T. Akamatsu, M. Kumazawa, N. Aikawa, and H. Takei, Phys. Chem. Miner. **19**, 431 (1993).

[9] F. Princivalle, Mineral. Petrol. **43**, 121 (1990).

[10] N. Aikawa, M. Kumazawa, and N. Tokonami, Phys. Chem. Miner. **12**, 1 (1985).

[11] R. M. Hazen, Am. Mineral **61**, 1280 (1976); Am. Mineral. **62**, 286 (1977).

[12] G. Will and G. Nover, Phys. Chem. Miner. **4**, 199 (1979); G. Nover and G. Will, Z. Kristallogr. **155**, 27 (1981); G. Ottonello, F. Princivalle, and A. Della Giusta, Phys. Chem. Miner. **17**, 301 (1990).

[13] V. Rajamani, G. E. Brown, and C. T. Prewitt, Am. Mineral. **60**, 292 (1975); A. G. Nord, H. Annersten, and A. Filippidis, *ibid.* **67**, 1206 (1982); H. R. Wenk and K. N. Raymond, Z. Kristal-

logr. **137**, 86 (1973).
[14] G. Artioli, R. Rinaldi, C. C. Wilson, and P. F. Zanazzi, Am. Mineral. **80**, 197 (1995); C. M. B. Henderson, K. S. Knight, S. A. T. Redfern, and B. J. Wood Science **271**, 1713 (1996); S. A. T. Redfern, G. Artioli, R. Rinaldi, C. M. B. Henderson, K. S. Knight, and B. J. Wood, Phys. Chem. Miner. **27**, 630 (2000).
[15] M. Morozov, C. Brinkmann, W. Lottermoser, W. Tippelt, G. Amthuer, and H. Kroll, Eur. J. Mineral. **17**, 495 (2005); M. N. Taran and M. Koch-Mller, Phys. Chem. Miner. **33**, 511 (2006).
[16] P. Hohenberg and W. Kohn, Phys. Rev. **136**, B864 (1964); W. Kohn and L. J. Sham, *ibid.* **140**, A1133 (1965).
[17] G. Kresse and J. Hafner, Phys. Rev. B **47**, 558 (1993); G. Kresse and J. Furthmüller, Comput. Mater. Sci. **6**, 15 (1996); G. Kresse and J. Furthmüller, Phys. Rev. B **54**, 11169 (1996).
[18] O. K. Andersen and O. Jepsen, Phys. Rev. Lett. **53**, 2571 (1984).
[19] P. E. Blöchl, Phys. Rev. B **50**, 17953 (1994); G. Kresse and D. Joubert, *ibid.* **59**, 1758 (1999).
[20] J. Hubbard, Proc. R. Soc. London, Ser. A **276**, 238 (1963).
[21] V. I. Anisimov, I. V. Solovyev, M. A. Korotin, M. T. Czyzyk, and G. A. Sawatzky, Phys. Rev. B **48**, 16929 (1993).
[22] L. Pisani and R. Valenti', Phys. Rev. B **71**, 180409(R) (2005).
[23] The obtained total-energy differences, computed for the whole cell, have been divided by the number of Fe atoms present in the unit cell so as to make the comparison between cases with different concentration of Fe atoms easier.
[24] S. A. T. Redfern, G. Artioli, R. Rinaldi, C. M. B. Henderson, K. S. Knight, and B. J. Wood, Phys. Chem. Miner. **27**, 630 (2000).
[25] H. T. Evans, Jr., J. S. Huebner, and J. A. Konnert, Earth Planet. Sci. Lett. **37**, 476 (1978).